 doi:10.20944/preprints202104.0274.v1

Article

Mechanical properties of glass-based geopolymer affected by activator and curing conditions under the optimal aging conditions

Tai-An Chen[1,*]

[1] Department of Harbor and River Engineering, National Taiwan Ocean University, No. 2, Pei-Ning Rd., Zhongzheng Dist., Keelung City 202301
* Correspondence: tachen@mail.ntou.edu.tw; Tel.: +886-2-2462-2192

Abstract: Inorganic polymeric materials react slowly at room temperature and as a result usually require high-temperature curing. This study used the Arrhenius equation to analyze the correlation between curing temperature and curing duration during high-temperature curing. The test results show that optimal values exist for each alkali equivalent of the activator (weight ratio of Na_2O/glass powder), curing temperature, and curing duration. Extending the curing duration and increasing the curing temperature have positive effects when the alkali equivalent is lower than the optimal value. However, over-curing results in invisible cracking in the specimens. Furthermore, despite exhibiting high strength initially, the strength of specimens gradually diminishes after standing in air. To ensure the durability of glass-based geopolymer, the curing temperature should not exceed 70℃, and the curing duration should be less than one day.

Keywords: Waste glass; Inorganic binder; Curing temperature; Curing duration

1. Introduction

The relentless usage of natural resources to fuel economic growth has given rise to the problem of shortages in many areas. As such, the reuse of waste products and environmentally friendly materials has become a growing international issue. Portland cement is the most used inorganic cementing material in civil engineering, but its production requires a process of grind once and burn twice, which needs a high temperature of 1300~1400℃ and produces a ton of carbon dioxide per ton of cement [1]. Indeed, global cement production has produced a total of 5-7% of the world's greenhouse gases [1, 2], still increasing at a 5% rate each year [1]. The development of a low-energy cost, low pollution inorganic cementing material as a replacement for Portland cement to protect the environment has thus become an important issue. Possible candidates for the task are alkali-activated binders.

Alkali-activated binder materials usually refer to cementing materials composed of aluminosilicates, alkaline solution, and alkali silicate solution. Aluminosilicates dissolve in strong alkaline solutions to release the required Si and Al elements, while aluminosilicates can supply sufficient amounts of silicate oligomer to improve the extent of polymerization of alkali-activated binders [3, 4], such as by increasing the strength and density of the microstructure. Alkali-activated binder materials are environmentally friendly, with a calcination temperature that is much lower than Portland cement's 1400 ℃, while also producing 20%-50% less CO_2 and consuming less energy [5]. Alkali-activated binder material is better with regard to weathering resistance, acid erosion and fire insulation compare to Portland cement, and is now used in fire insulation, waste solidification, and structural materials, among other applications [6-9].

Preprints (www.preprints.org) | NOT PEER-REVIEWED | Posted: 12 April 2021 doi:10.20944/preprints202104.0274.v1

The raw materials of alkali-activated cementitious materials are varied, such as metakaolin [7, 10], GGBFs [11], fly ash [12], silica fume [13], bottom ash [14], graphene oxide [15], construction and demolition waste [16], eggshell powder [17], and calcined reservoir sludge [18], and mixing with an activator which is usually composed of alkali metal hydroxide and sodium silicate. In the alkali-activation reaction of inorganic polymers, the dissolution of the ions in aluminosilicate minerals is mainly caused by alkali metal hydroxide, while the subsequent polycondensation of some silicate precursors is partially caused by sodium silicate. Thus, compared to Portland cement, the compressive strengths of inorganic binders would be much better due to the contribution of mixing with activators of sodium hydroxide and sodium silicate

As such, alkali-activated inorganic binders are categorized into two types according to their microstructures. One is alkali-activated slag, denoted by AAS, having a microstructure with a low Ca/Si ratio C-S-H gel [19]. Another one is alkali-activated metakaolin or Class-F fly ash with a colloidal microstructure of tetrahedron SiO_4 and AlO_4^- [20, 21].

Binders composed of waste products must have lower manufacturing costs if they are to be competitive. As such, this research utilizes 100% waste glass to create a binder while looking for a better composition to further reduce the cost of using activators and improving the material properties of the alkali-activated binder. Habert et al. suggested that using industrial waste with a suitable molar ratio to reduce the amount of sodium silicate required in activators. Because the productions of sodium silicate has even worse impacts on the environment than ordinary Portland cement [22]. Waste glass has the characteristic which is mentioned above and there are also relative researches taking glass to be as a geopolymer. Luhar et al. compiled serval references on the effects of glass applied to geopolymer on durability, thermal and microstructural properties [23]. Christiansen discussed the influence of different types of glass and alkali activators on the properties of geopolymers [24]. Chen et al. [25] proposed an aging process to make glass-based geopolymer, and its mechanical properties are equivalent to those without silicate solution. In addition, changing the curing conditions can also enhance the mechanical properties of glass-based geopolymers [26]. This study uses waste glass as an activator to replace sodium silicate, which is expensive and environmentally unfriendly and is also based on Chen et al. [25]; by changing the curing conditions under the optimal aging conditions to discuss if the adjustment of temperature and time during the curing stage can produce higher performance glass-based geopolymer. In addition, according to the study of concrete, its durability, bending strength, and shear strength are correlated to the compressive strength. Therefore, this study measured the compressive strength of glass-based geopolymer.

2. Materials and Methods

2.1. Raw materials

To use waste glass containers as the raw material for producing geopolymer has to go through the following steps after picking them up and bring back to the laboratory from the resource recycling plant. First, clean the glass bottles and then dry them in the air. Next, crush them to a particle size under 300μm, and use a pan mill to make the crushed glass bottles ground into glass powder. The physical and chemical properties of the glass powder are shown in Table 1. According to the XRD patterns of glass powder shown in Figure 1, obtained by scanning at 2θ/min, and the scanning range was 10°–80°, highly amorphous state characteristics of glass powder can be seen. Through the physical and chemical properties and its XRD patterns show that glass powder has high content of reactive silica which is one of the most important factors in geopolymer formation is reactive silica. To sum up, glass powder can be used to replace sodium silicate in the preparation of geopolymers.

Table 1. Physical and chemical properties of waste glass

Preprints (www.preprints.org) | NOT PEER-REVIEWED | Posted: 12 April 2021 doi:10.20944/preprints202104.0274.v1

SiO_2	Al_2O_3	Fe_2O_3	CaO	MgO	Na_2O	K_2O	G_s	Absorption	Specific surface area
72.5%	2%	0.06%	10.5%	1%	13%	0.5%	2.55	0.2%	4303 cm^2/g

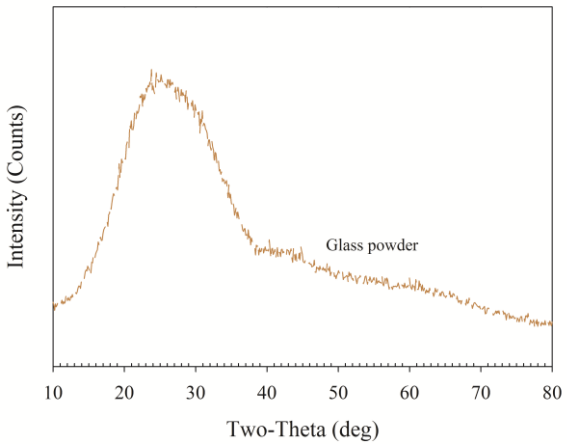

Figure 1. XRD patterns of container waste glass.

2.2. Activator

Use two typical parameters to discuss the effect of activator, one is alkali-equivalent content and the other is water/binder ratio. The alkali-equivalent content, represented as AE%, is defined as the weight fraction of Na_2O to glass powders. The water/binder ratio, written as W/B, is the weight ratio of water to the summation of glass powders, and sodium hydroxide in an activator. The sodium hydroxide was produced by ECHO Chemical Co., LTD. and had 99% purity. In this study, W/B was fixed at 0.3 for all glass-based geopolymer specimens. The mix proportions of the studied glass-based geopolymer specimens with AE% = 1-6% are listed in **Table 2** respectively.

Table 2. The mix proportions of the glass-based geopolymer specimens with AE% = 1-6%.

W/B	AE%	Sodium hydroxide (g)	Water (g)	Glass powder (g)
0.3	1%	12.91	303.87	1000
	2%	25.82	307.75	1000
	3%	38.73	311.62	1000
	4%	51.64	315.49	1000
	5%	64.55	319.37	1000
	6%	77.47	323.24	1000

2.3. Aging process

In the aging process, sodium hydroxide served as the activator in the aging process. The sodium hydroxide was mixed thoroughly with water, and then the alkali solution was set to cool to room temperature. Next, we heated the bath tank to the preset aging temperature using a temperature-controlled heating device and poured the glass powder and alkali activator mixture into a sequencing batch reactor. Mixing was first conducted at room temperature at 500 rpm for 30 seconds using a DC mixer. We then covered the mixture with plastic wrap and placed it into a water bath to hold the temperature. Mixing continued at 500 rpm with the DC mixer until the preset time, after which the mixture was poured into 3cm×3cm×3cm three-gang cube molds in two layers. The mixtures were tamped using a vibration table (Italy CONTROLS, frequency: 60 Hz) to remove any bubbles within the specimens. We adopted the following aging times for alkali equiva-

Preprints (www.preprints.org) | NOT PEER-REVIEWED | Posted: 12 April 2021 doi:10.20944/preprints202104.0274.v1

lents AE%=1%-6% below the aging temperature of 70℃: 105 min, 55 min, 40 min, 35 min, 35 min, and 25 min [25].

2.4. Curing process

To prevent moisture loss, we wrapped the specimens with plastic film and then placed the specimens, including the mold, into an oven, to cure for the preset time period. The specimens were removed from the oven and demold once they had cooled to room temperature. Then they stood at room temperature for 4 days. The curing temperatures for each glass slurry and alkali equivalent included 60℃, 70℃, 80℃, 90℃, and 100℃. The curing durations were increased by 8 hours until reaching 4 days. For instance, a curing duration of 8 hours meant that the specimens were in the oven for 8 hours and then stood at room temperature after demolding for 88 hours. This was 4 days in total, at which time the compressive strength of the specimens was measured. The compressive strength of the specimens was measured using a Shimadzu UHC-100A universal tester with a constant loading speed of 300 KPa/s for stress control.

2.5. Specimen strength development

To understand the strength development of the specimens about curing temperature and period, we performed the following tests. For curing temperature, we tested the compressive strength of specimens with alkali equivalents 3% and 6%, curing duration 24 hours, standing time 0 days, 7 days, 14 days, 21 days, and 28 days, and curing temperatures between 60℃ and 100℃. For curing duration, we tested the compressive strength of specimens with curing temperature 70℃, curing durations 8, hours, 16 hours, 24 hours, 48 hours, and 96 hours, and standing time 0 days, which means that the compressive strength of the specimens was measured once they had cooled to room temperature (approximately 1 hour). For the remaining curing durations, we measured compressive strength after letting the specimens stand in the air for the corresponding period.

3. Results and discussion

3.1. Effects of alkali equivalent on curing process

Table 3 presents the curing conditions corresponding to the optimal compressive strength for each alkali equivalent. As can be seen, at the same curing temperature, a higher alkali equivalent results in a shorter optimal curing duration for the glass-based geopolymer. For instance, with a curing temperature of 80℃, the optimal curing duration is 64 hours when the alkali equivalent is 1% and shortens to 48 hours and 40 hours when the alkali equivalent is 3% and 6%, respectively. However, regardless of the curing conditions, the final approximate compressive strength is controlled by the alkali equivalent, with the exception of curing temperature 60℃ paired with alkali equivalents 1% and 2%, in which 4 days was not adequate for the specimens to reach their ultimate compressive strength (marked with <> in Table 3). We speculate that by extending the curing time, the approximate ultimate compressive strength can be reached. During the curing period, the water molecules and the OH^- ions may diffuse to the surface of undissolved glass particles and continue to corrode them [27]. The greater the alkali equivalent is, the more vigorous this reaction is. Extending the curing period means that the remaining OH^- ions will corrode the polymerized glass-based geopolymer, which reduces the strength. In other words, high-temperature curing can be regarded as an extension of the aging process, which means that lower alkali equivalents will require higher curing temperatures or longer curing durations.

Table 3. Ultimate compressive strengthes under various curing temperatures when AE%=1-6%.

	AE% = 1%	**AE% = 2%**	**AE% = 3%**

Preprints (www.preprints.org) | NOT PEER-REVIEWED | Posted: 12 April 2021 doi:10.20944/preprints202104.0274.v1

Curing Temperature (℃)	Curing Duration (hr)	Compressive Strength (MPa)	Curing Duration (hr)	Compressive Strength (MPa)	Curing Duration (hr)	Compressive Strength (MPa)
60	96	<55.24>	96	<76.26>	96	129.65
70	88	71.97	88	106.72	80	136.77
80	64	69.53	48	101.89	48	129.97
90	48	69.96	32	85.89	32	126.83
100	24	65.31	24	82.31	24	96.21
Ultimate compressive strength		69.19		94.20		123.89
	AE% = 4%		**AE% = 5%**		**AE% = 6%**	
Curing Temperature (℃)	**Curing Duration (hr)**	**Compressive Strength (MPa)**	**Curing Duration (hr)**	**Compressive Strength (MPa)**	**Curing Duration (hr)**	**Compressive Strength (MPa)**
60	96	122.62	88	119.25	88	108.17
70	64	119.65	64	107.96	56	103.60
80	48	105.34	48	114.84	40	115.91
90	32	103.05	32	100.72	24	109.37
100	16	111.24	16	97.01	8	96.86
Ultimate compressive strength		112.38		107.96		106.78

3.2. Effects of curing temperature on compressive strength

Observation of **Figure** 2-4 show that prior to reaching the optimal alkali equivalent of 3% and with fixed curing time at 24 hours and curing temperatures 60℃, 70℃, 80℃, 90℃, and 100℃, the compressive strength of the glass-based geopolymer increases with the curing temperature. When AE%=1%, the compressive strength increases from 25.87 MPa to 65.31 MPa; when AE%=2%, the compressive strength increases from 44.56 MPa to 82.31 MPa, and when AE%=3%, the compressive strength increases from 85.85 MPa to 96.21 MPa. When the curing duration is extended to 48 hours, AE%=1% results in an optimal compressive strength of 69.96 MPa at 90℃, whereas with AE%=2% and AE%=3%, the optimal curing temperature is 80℃, resulting in compressive strength 101.89 MPa and 129.97 MPa, respectively.

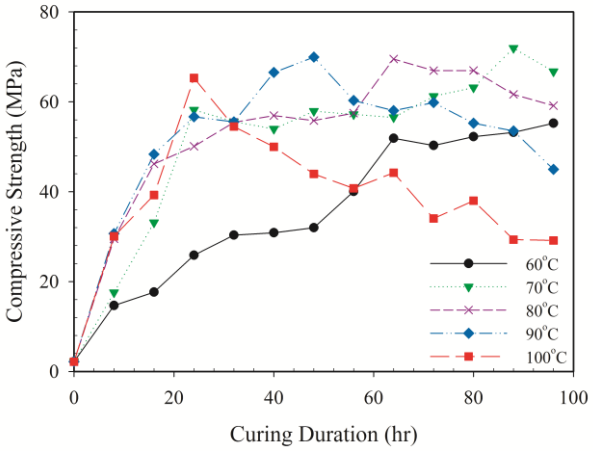

Figure 2. Variations of four-day compressive strength of glass-based geopolymers with curing duration in varied curing temperatures at AE% = 1%.

Preprints (www.preprints.org) | NOT PEER-REVIEWED | Posted: 12 April 2021 doi:10.20944/preprints202104.0274.v1

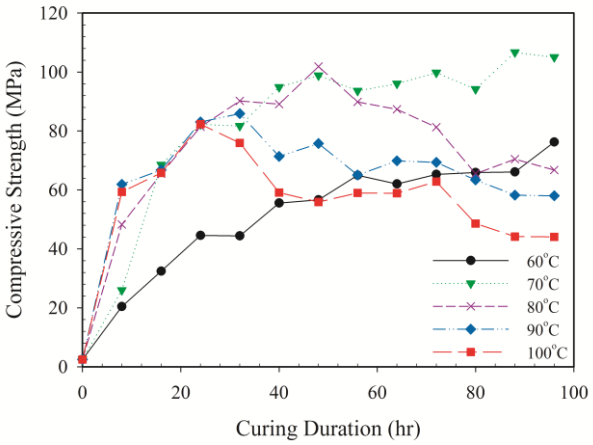

Figure 3. Variations of four-day compressive strength of glass-based geopolymers with curing duration in varied curing temperatures at AE% = 2%.

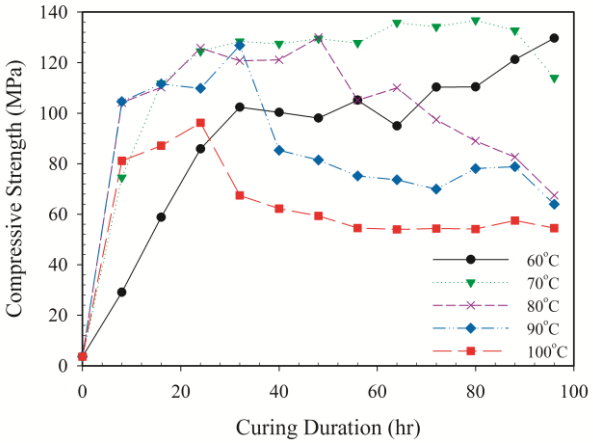

Figure 4. Variations of four-day compressive strength of glass-based geopolymers with curing duration in varied curing temperatures at AE% = 3%.

Figure 5-7 present the results from various temperatures when the optimal alkali equivalent of 3% is exceeded. With AE%=4-6%, the curing duration fixed at 24 hours, and curing temperatures 60℃, 70℃, 80℃, 90℃, and 100℃, the comprehensive strength of the glass-based geopolymer specimens increases with the temperature between 60℃ and 90 ℃, rising from 73.16 MPa to 94.09 MPa, from 77.19 MPa to 83.28 MPa, and from 72.84 MPa to 109.37 MPa, respectively. However, when the curing temperature increases to 100 ℃, the compressive strength of the specimens instead drops to 88.64 MPa, 71.13 MPa, and 71.98 MPa. When the curing duration is extended to 48 hours, AE%=5% and AE%=6% results in the compressive strength increasing with curing temperature between 60℃ and 80℃ but decreasing with curing temperature between 80℃ and 100℃. For instance, when AE%=5%, the compressive strength of the glass-based geopolymer first increases from 98.80 MPa to 114.84 MPa and then decreases to 55.02 MPa. In contrast, when AE%=6%, the compressive strength of the glass-based geopolymer between 60℃ and 80 ℃ remains relatively constant (95.82 MPa, 92.59 MPa, and 94.03 MPa, respectively).

Preprints (www.preprints.org) | NOT PEER-REVIEWED | Posted: 12 April 2021 doi:10.20944/preprints202104.0274.v1

When the curing temperature rises to 100℃, the compressive strength drops to 49.27 MPa.

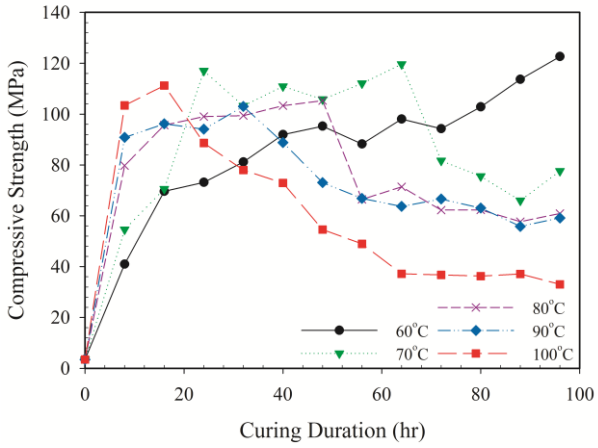

Figure 5. Variations of four-day compressive strength of glass-based geopolymers with curing duration in varied curing temperatures at AE% = 4%.

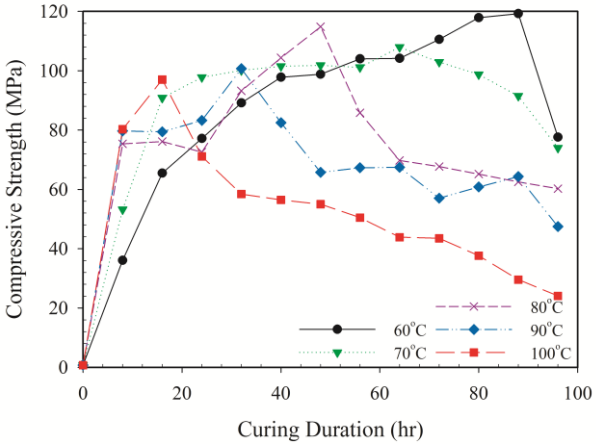

Figure 6. Variations of four-day compressive strength of glass-based geopolymers with curing duration in varied curing temperatures at AE% = 5%.

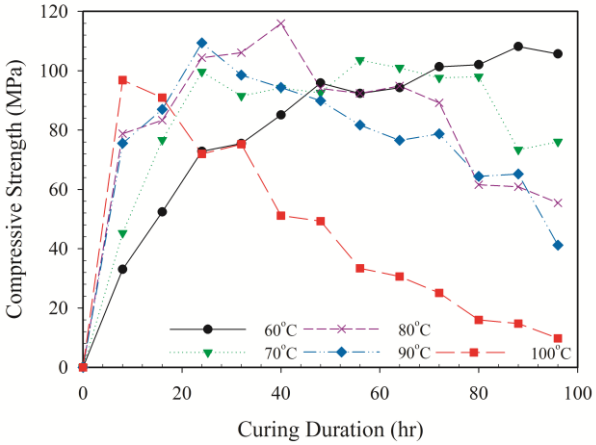

Figure 7. Variations of four-day compressive strength of glass-based geopolymers with curing duration in varied curing temperatures at AE% = 6%.

 doi:10.20944/preprints202104.0274.v1

In **Figure** 2-7, the compressive strength curves of the glass-based geopolymer specimens become steeper as the curing temperature rises, regardless of the alkali equivalent. The optimal curing temperature declines with AE%, which means that increasing the curing temperature can accelerate the rate at which the glass slurry solidifies. However, if the curing temperature continues to rise, the compressive strength then declines.

3.3. Effects of curing duration on compressive strength

Figure 2-7 shows the relationship between compressive strength and curing duration in the glass-based geopolymer specimens at various curing temperatures. As can be seen, the compressive strength increases with the curing duration until the optimal curing time is reached, after which the compressive strength decreases with the curing duration. With curing temperature 80℃, AE%=1-3%, and the curing duration under 24 hours, the compressive strength of the specimens increases significantly with the curing duration, from 2.18 MPa, 2.44 MPa, and 3.62 MPa to 50.12 MPa, 81.45 MPa, and 125.79 MPa, respectively. When the curing duration extends beyond 24 hours, the increasing influence of the curing duration on compressive strength is greatly mitigated, resulting in compressive strength of 69.53 MPa, 101.89 MPa, and 129.97 MPa at curing durations of 64 hours, 48 hours, and 48 hours, respectively. Once the curing duration has been lengthened to 4 days, the compressive strength decreases to 59.18 MPa, 66.78 MPa, and 67.45 MPa. The specimens with AE%=4-6% display the same trend. For example, with a curing temperature of 70℃ and curing durations of under 24 hours, the compressive strength of the specimens increases significantly with the curing duration, from 3.47 MPa, 0.71 MPa, and no strength to 117.01 MPa, 97.81 MPa, and 99.66 MPa. When the curing duration extends beyond 24 hours, the influence of curing duration on compressive strength is greatly mitigated, resulting in compressive strength 119.65 MPa, 107.96 MPa, and 103.60 MPa at curing durations of 64 hours, 64 hours, and 56 hours, respectively. Once the curing duration has been lengthened to 4 days, the compressive strength decreases to 77.61 MPa, 73.98 MPa, and 76.07 MPa.

Except for the specimens cured at 60℃, the specimens with AE%=1-5% all continued to increase in strength for the first 4 days. Regardless of curing temperature or period, the curing process of the glass-based geopolymer can be roughly divided into three phases. During the first phase, the polymerization reaction of the glass is vigorous, and the amount of consolidated colloid increases considerably, thereby providing strength. During the second phase, the compressive strength of the glass-based geopolymer increases slightly with the curing duration. The low alkali and temperatures necessitate a longer period of time, which created a clear distinction between the first and second phases. As the alkali equivalent and curing temperature increase, the second phase becomes less distinguishable. Finally, the third phase lengthens the glass consolidation period but the compressive strength of glass-based geopolymer decreases. Over-curing leads to thermal cracking in the specimens, which in turn affect their performance and compressive strength.

3.4. Effects of curing process on long-term strength development

Section 3.2. shows that increasing the curing temperature can shorten the curing duration. However, to understand the strength development of glass-based geopolymer placed in the air following various curing conditions, we examined the strength development of specimens with AE%=3% and AE%=6%, various curing temperatures, and a curing duration of 24 hours as well as the strength development of specimens with a curing temperature of 70℃, curing durations of 8 hours, 16 hours, 24 hours, 48 hours, and 96 hours, and standing time of 28 days.

Preprints (www.preprints.org) | NOT PEER-REVIEWED | Posted: 12 April 2021 doi:10.20944/preprints202104.0274.v1

As shown in the results in **Figure** 8 and **Figure** 9, the specimen with AE%=3%, curing temperature of 100℃, and curing duration of 24 hours attained greater comprehensive strength (121.30 MPa) than the specimens cured at other temperatures after cooling for 1 hour in the air. However, after standing in air for 28 days, this specimen has the weakest compressive strength (51.14 MPa). In contrast, the specimen cured at 70℃ only attains compressive strength of 97.75 MPa after cooling in the air for 1 hour, but after 28 days, its strength increases to 121.93 MPa. Among specimens with AE%=6%, the specimen cured at 80℃ displayed the highest strength of 83.50 MPa immediately after curing. The specimen cured at 60℃ presented the highest strength of 96.08 MPa after standing in air for 28 days. This shows that an overly high curing temperature can have adverse effects on glass-based geopolymer. We speculate that only some, not all, of the material rapidly solidifies within a short period of time. After standing in the air, cracks form between regions, thereby reducing the strength.

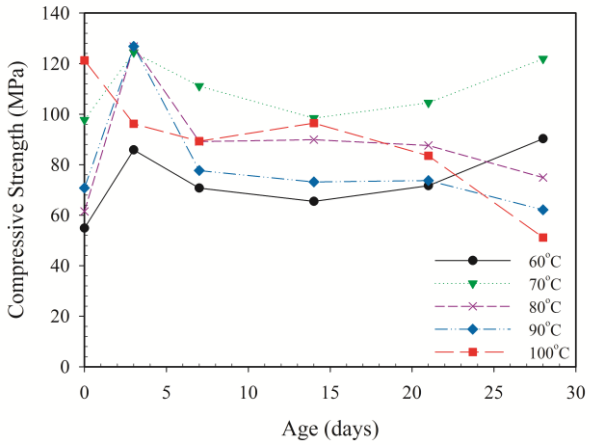

Figure 8. Chang in compressive strength with age in the air under various curing temperature after 24-hour oven curing with AE% = 3%.

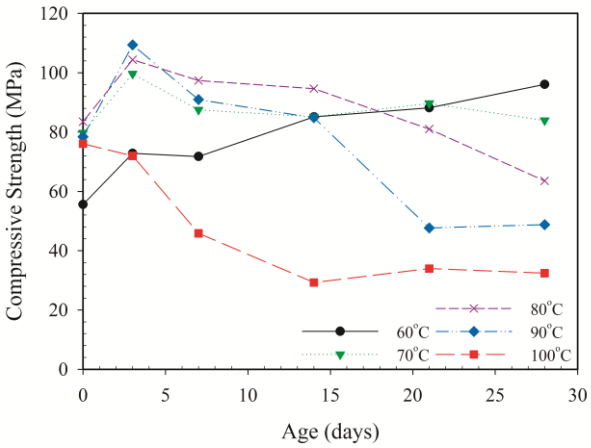

Figure 9. Chang in compressive strength with age in the air under various curing temperature after 24-hour oven curing with AE% = 6%.

Figure 10 and **Figure** 11 exhibit the strength development of the specimens standing in the air after curing durations of varying lengths. Among specimens with AE%=3%, the specimen cured for 24 hours showed the highest compressive strength of 121.93 MPa after standing in air for 28 days. In contrast, the specimen cured for 96 hours showed the highest compressive strength of 120.75 MPa immediately after curing. Among speci-

Preprints (www.preprints.org) | NOT PEER-REVIEWED | Posted: 12 April 2021 doi:10.20944/preprints202104.0274.v1

mens with AE%=6%, the specimen cured at 70℃ for 48 hours showed the highest compressive strength of 100.37 MPa. In contrast, the specimen cured for 24 hours showed the highest compressive strength of 83.93 MPa after standing in air for 28 days. These results show that the curing duration must be precisely the right length for the glass slurry to dehydrate into an glass-based geopolymer. Excessive thermal energy will damage micro-structures over the long term.

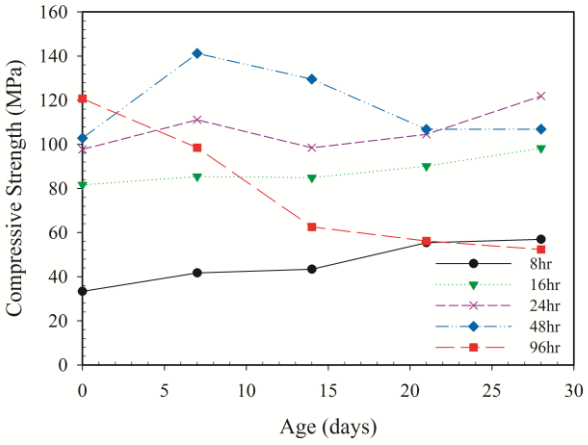

Figure 10. Change in compressive strength change with age in the air under various curing durations in 70℃ oven curing with AE% = 3%.

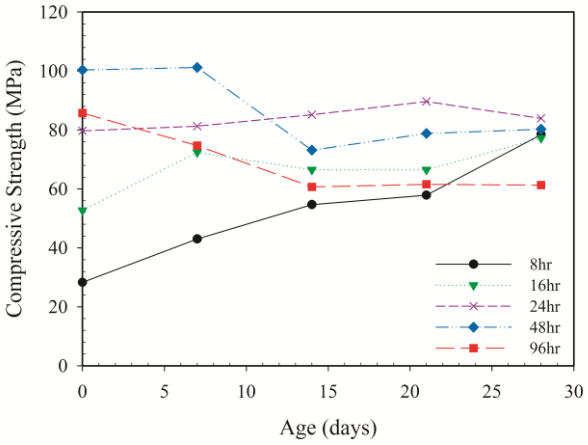

Figure 11. Change in compressive strength change with age in the air under various curing durations in 70℃ oven curing with AE% = 6%.

4. Conclusions

The objective of this study was to compressive strength in the high-temperature curing of glass-based geopolymer under optimal aging process. Test results demonstrate that the strength of glass-based geopolymer is associated with its solidification. Extending the curing duration and increasing the curing temperature can facilitate the strength development of glass-based geopolymer specimens. However, over-curing results in thermal cracking that reduce the compressive strength. The most suitable curing temperature and period are determined by the alkali equivalent. Higher alkali equivalents require shorter curing durations and lower curing temperatures. The ultimate compressive strength is not influenced by the curing duration and temperature but is controlled by the alkali equivalent.

Overly high curing temperatures and overly long curing durations have adverse effects on specimen strength in the long term. The former has a particularly severe impact, so it is suggested that the curing temperature does not exceed 70℃. Furthermore, curing durations under 24 hours will enable the strength to develop gradually. Overly high curing temperatures or overly long curing durations will only cause the strength to decline.

Funding: This research received no external funding.

Conflicts of Interest: The author does not have any conflicts of interest with another.

References

1. Davidovits, J. Geopolymer cements to minimise carbon-dioxide greenhouse-warming, *Ceram. Trans.* **1993**, 37, 165-182.
2. Mehta, P.K. Reducing the environmental impact of concrete, *Concr. Int.* **2001**, 23(10), 61-66.
3. Xu, H.; Van Deventer, J.S.J. The geopolymerisation of alumino-silicate minerals, *Int. J. Miner. Process.* **2000**, 59(3), 247-266. doi.org/10.1016/S0301-7516(99)00074-5
4. Krizan, D.; Zivanovic, B. Effects of dosage and modulus of water glass on early hydration of alkali–slag cements, *Cem. Concr. Res*. **2002**, 32(8), 1181-1188. doi.org/10.1016/S0008-8846(01)00717-7
5. Davidovits, J. Geopolymers: man-made rock geosynthesis and the resulting development of very early high strength cement, *J. Mater. Educ.* **1994**, 16, 91-139.
6. Davidovits. J. 30 years of successes and failures in geopolymer applications. Market trends and potential breakthroughs. Keynote Conference on Geopolymer Conference. 2002.
7. Davidovits, J. Geopolymers: Inorganic polymeric new materials, *J. Therm. Anal.* **1991**, 37(8), 1633-1656. doi.org/10.1007/bf01912193
8. Wang, S.D.; Pu, X.C.; Scrivener, K.; Pratt, P.L. Alkali-activated slag cement and concrete: a review of properties and problems, *Adv. Cem. Res.* 1995, 7(27), 93-102. doi.org/10.1680/adcr.1995.7.27.93
9. Roy, D.M. Alkali-activated cements opportunities and challenges, *Cem. Concr. Res.* **1999**, 29(2), 249-254. doi.org/10.1016/S0008-8846(98)00093-3
10. Medri, V., E. Papa, J. Lizion and E. Landi. Metakaolin-based geopolymer beads: Production methods and characterization, *J. Clean. Prod* **2019**, 244, 118844. doi:10.1016/j.jclepro.2019.118844.
11. Ez-zaki, H.; Bellotto, M.; Valentini, L.; Garbin, E.; Artioli, G. Influence of cellulose nanofibrils on the rheology, microstructure and strength of alkali activated ground granulated blast-furnace slag: a comparison with ordinary Portland cement. *Mater Struct* **2021**, 54(1), 1-18. doi.org/10.1617/s11527-020-01614-5
12. Atiş, C. D.; Görür, E. B.; Karahan, O.; Bilim, C.; Ilkentapar, S.; Luga, E. Very high strength (120 MPa) class F fly ash geopolymer mortar activated at different NaOH amount, Heat Curing Temperature and Heat Curing Duration, *Constr Build Mater.* **2015,** 96, 673-678. doi:10.1016/j.conbuildmat.2015.08.089.
13. Bahrami, M.; Shalbafan, A.; Welling, J. Development of plywood using geopolymer as binder: effect of silica fume on the plywood and binder characteristics. *EUR J Wood PROD* **2019**, 77(6), 981-994. doi.org/10.1007/s00107-019-01462-3.
14. Chindaprasirt, P.; Jaturapitakkul, C.; Chalee, W.; Rattanasak, U. Comparative study on the characteristics of fly ash and bottom ash geopolymers, *Waste Manage.* **2009**, 29(2), 539-543. doi.org/10.1016/j.wasman.2008.06.023
15. Sun, Q.; Liu, J.; Cheng, H.; Mou, Y.; Liu, J.; Peng, Y.; Chen, M. Fabrication of 3D structures via direct ink writing of kaolin/graphene oxide composite suspensions at ambient temperature. *Ceram. Int.* **2019**, 45(15), 18972-18979. doi.org/10.1016/j.ceramint.2019.06.136
16. Lampris, C.; Lupo, R.; Cheeseman, C.R. Geopolymerisation of silt generated from construction and demolition waste washing plants, *Waste Manage.* **2009**, 29(1), 368-373. doi.org/10.1016/j.wasman.2008.04.007
17. Shekhawat, P.; Sharma, G.; Singh, R.M. Strength behavior of alkaline activated eggshell powder and flyash geopolymer cured at ambient temperature. *Constr Build Mater.* **2019**, 223, 1112-1122. doi.org/10.1016/j.conbuildmat.2019.07.325
18. Yang, K.H.; Lo, C.W.; Huang, J.S. Production and properties of foamed reservoir sludge inorganic polymers, *Cem. Concr. Compos.* **2013**, 38, 50-56. doi.org/10.1016/j.cemconcomp.2013.03.017
19. Dung, N.T.; Chang, T.P.; Chen, C.T.; Yang, T.R. Cementitious properties and microstructure of an innovative slag eco-binder, *Mater Struct* **2016**, 49(5), 2009-2024. doi:10.1617/s11527-015-0630-6.
20. Mehta, A.; Siddique, R. Properties of low-calcium fly ash based geopolymer concrete incorporating OPC as partial replacement of fly ash, *Constr Build Mater.* **2017**, 150(1), 792-807. doi:10.1016/j.conbuildmat.2017.06.067.
21. Nguyen, H.A.; Chang, T.P.; Shih, J.Y.; Chen, C.T. Influence of low calcium fly ash on compressive strength and hydration product of low energy super sulfated cement paste, *Cem. Concr. Compos.* **2019**, 99, 40-48. doi: 10.1016/j.cemconcomp.2019.02.019.
22. Habert,G.; d'Espinose de Lacaillerie, J.B.; Roussel, N. An environmental evaluation of geopolymer based concrete production: reviewing current research trends, *J. Clean. Prod* **2011**, 19(11), 1229-1238. doi.org/10.1016/j.jclepro.2011.03.012

23. Luhar, S.; Cheng, T.W.; Nicolaides, D.; Luhar, I.; Panias, D.; Sakkas, K. Valorisation of glass wastes for the development of geopolymer composites–Durability, thermal and microstructural properties: A review. *Constr Build Mater.* **2019**, 222, 673-687. doi.org/10.1016/j.conbuildmat.2019.06.169
24. Christiansen, M.U. Effects of Composition and Activator Type on Glass-Based Geopolymers. *ACI Mater. J.* **2019**, 116(5), 239-250. doi:10.14359/51716979.
25. Chen, T.A.; Chen, J.H.; Huang, J.S. Effects of activator and aging process on the compressive strengths of alkali-activated glass inorganic binders. *Cem. Concr. Compos.* **2017**, 76, 1-12. doi.org/10.1016/j.cemconcomp.2016.11.011
26. Chen, T.A. Optimum curing temperature and duration of alkali-activated glass inorganic binders. *J CHIN INST ENG* **2020**, 43(6), 592-602. doi.org/10.1080/02533839.2020.1777206
27. Hosoi, K.; Kawai, S.; Yanagisawa, K.; Yamasaki, N. Densification process for spherical glass powders with the same particle size by hydrothermal hot pressing, *J. Mater. Sci.* **1991**, 26(23), 6448-6452. doi.org/10.1007/BF00551895